



# OPEN MiR-340-5p regulates PD-L1 and predicts pembrolizumab response in extranodal NK/T-cell lymphoma

Kyung Ju Ryu<sup>1,4</sup>, Haein Ji<sup>1,4</sup>, Bon Park<sup>1</sup>, Sang Eun Yoon<sup>2</sup>, Junhun Cho<sup>3</sup>, Won Seog Kim<sup>1,2</sup>, Hyeon Ho Kim<sup>1</sup>✉ & Seok Jin Kim<sup>1,2</sup>✉

Extranodal NK/T-cell lymphoma (ENKTL) is an aggressive, chemoresistant non-Hodgkin lymphoma subtype with poor patient outcomes linked to elevated PD-L1 expression. This study investigates miRNA-mediated regulation of PD-L1, focusing on miR-340-5p and miR-424-5p as novel therapeutic targets and predictive biomarkers for pembrolizumab response. Through miRNA sequencing and functional assays, miR-340-5p and miR-424-5p were identified as key modulators of PD-L1 in drug-resistant ENKTL cells, with their roles validated via ribonucleoprotein immunoprecipitation and luciferase reporter assays. Notably, elevated miR-340-5p levels in PD-L1-negative ENKTL tissues were inversely correlated with soluble PD-L1, implicating miR-340-5p in immune evasion mechanisms. Additionally, low serum levels of miR-340-5p were associated with reduced pembrolizumab efficacy, positioning miR-340-5p as a promising predictive biomarker for immune checkpoint blockade. These findings suggest that pre-treatment assessment of serum miR-340-5p could guide pembrolizumab therapy in ENKTL, optimizing treatment outcomes. Validation in larger cohorts is necessary to confirm the utility of miR-340-5p as a predictive biomarker for ENKTL immunotherapy.

**Keywords** PD-L1, miR-340-5p, NK/T-cell Lymphoma, Biomarkers

Extranodal natural killer/T-cell lymphoma (ENKTL) is a rare and aggressive form of non-Hodgkin lymphoma that originates from either natural killer (NK) or cytotoxic T cells and is linked with Epstein-Barr virus (EBV) infections<sup>1</sup>. The presence of EBV in lymphoma cells is associated with the upregulation of programmed death ligand 1 (PD-L1), which binds to programmed cell death protein 1 (PD-1) on effector T cells<sup>2</sup>. This interaction leads to T-cell exhaustion and hampers the immune system's ability to combat the tumor. Consequently, blocking the PD-1/PD-L1 pathway is seen as a promising therapeutic approach to enhance T-cell cytotoxicity against the tumor. Immune checkpoint inhibitors, such as pembrolizumab and nivolumab, which target PD-1, have demonstrated potential in interrupting this interaction and offer therapeutic advantages in various cancers, including hematologic malignancies<sup>3</sup>. Specifically, pembrolizumab is considered an effective treatment option for patients with relapsed or refractory ENKTL<sup>4,5</sup>. However, not all patients with ENKTL respond, and ENKTL also can progress or relapse during or after treatments with immune checkpoint inhibitors. This highlights the challenge of immune checkpoint inhibitor resistance and underscore the urgent need for biomarkers predicting the risk of treatment failure after immune checkpoint inhibitors in ENKTL patients.

Our previous research indicated that serum soluble PD-L1 levels were elevated in patients with relapsed or refractory ENKTL compared to healthy controls. Notably, these levels were significantly lower in patients who responded to pembrolizumab treatment than in those who did not, suggesting that soluble PD-L1 may interfere with the binding of PD-1 inhibitors to PD-L1 on tumor cells<sup>6</sup>. It is hypothesized that soluble PD-L1 originates from PD-L1-positive cells, including tumor cells, and that exosomes released from these cells may contribute to its presence in the serum<sup>7,8</sup>. Although it is established that EBV infection prompts PD-L1 expression in ENKTL, and all tumor cells in these patients tested positive for EBV, the expression levels of PD-L1 varied among individuals. However, data on the factors that regulate both PD-L1 and soluble PD-L1 expression in ENKTL are sparse, making it challenging to fully understand the mechanisms behind PD-L1 expression in this context.

<sup>1</sup>Department of Health Sciences and Technology, Samsung Advanced Institute of Health Sciences and Technology, Sungkyunkwan University, 81 Irwon-ro Gangnam-gu, Seoul 06351, Korea. <sup>2</sup>Division of Hematology-Oncology, Department of Medicine, Samsung Medical Center, Sungkyunkwan University School of Medicine, 81 Irwon-ro Gangnam-gu, Seoul 06351, Korea. <sup>3</sup>Department of Pathology, Samsung Medical Center, Sungkyunkwan University School of Medicine, Seoul, Korea. <sup>4</sup>Kyung Ju Ryu and Haein Ji contributed equally to this work. ✉email: hyeonhkim@skku.edu; kstwh@skku.edu

MicroRNAs (miRNAs) are small, non-coding RNA molecules that play crucial roles in regulating gene expression and are involved in various cellular processes including proliferation, apoptosis, differentiation, and immune responses. These processes encompass the modulation of immune checkpoints such as PD-L1, which is pivotal in tumor immune evasion<sup>9</sup>. Recent research has highlighted specific miRNAs, such as miR-34a, miR-200b, miR-197, miR-513, and miR-138-5p, as regulators of PD-L1 expression in cancer cells, potentially impacting the effectiveness of immunotherapy. These miRNAs could also act as surrogate biomarkers for PD-L1 expression<sup>10–13</sup>. Despite these insights, there remains a gap in identifying specific miRNA biomarkers that can predict responses of ENKTL patients to immune checkpoint inhibitors. This study aims to explore the potential of miRNAs as predictive biomarkers for such therapies in ENKTL patients. We report on the involvement of miRNA in PD-L1 expression and its correlation with responses to pembrolizumab, thereby opening up new avenues for targeted therapeutic strategies in this complex malignancy.

## Results

### Mechanisms of PD-L1 regulation in etoposide-resistant ENKTL cells

In our previous study, we developed an etoposide-resistant ENKTL cell line (SNK6R) that demonstrated a notable resistance to etoposide, a primary chemotherapeutic used in ENKTL treatment (Fig. 1A)<sup>14</sup>. Interestingly, these cells also exhibited a significant increase in PD-L1 expression compared to the parental SNK6 cells (Fig. 1B). To explore the underlying mechanisms, we employed Ago2 RNP-IP, which showed that the enrichment of PD-L1 mRNA in Ago2 IP was higher in parental cells than in resistant cells (Fig. 1C). This finding indicates the possibility that miRNA is involved in the upregulation of PD-L1 in resistant cells. To further investigate, we performed miRNA sequencing on SNK6 and SNK6R cells to identify specific miRNAs that regulate PD-L1 expression. This analysis identified 18 downregulated and 10 upregulated miRNAs relative to the parental SNK6 cells. Notably, six miRNAs—miR-30d-3p, miR-148a-3p, miR-221-5p, miR-340-5p, miR-378a-3p, and miR-424-5p—were significantly downregulated in the drug-resistant cells and predicted to target PD-L1 mRNA via TargetScan (Fig. 1D). We validated the expression of these miRNAs using RT-qPCR and Western blotting in both SNK6R and control SNK6 cells. The results confirmed that these miRNAs were indeed lower in SNK6R cells compared to controls, with the exception of miR-221-5p (Fig. 1E). Further analysis through Western blotting demonstrated that specifically miR-340-5p and miR-424-5p downregulate PD-L1 expression, indicating their pivotal role in modulating PD-L1 in the context of drug resistance (Fig. 1F).

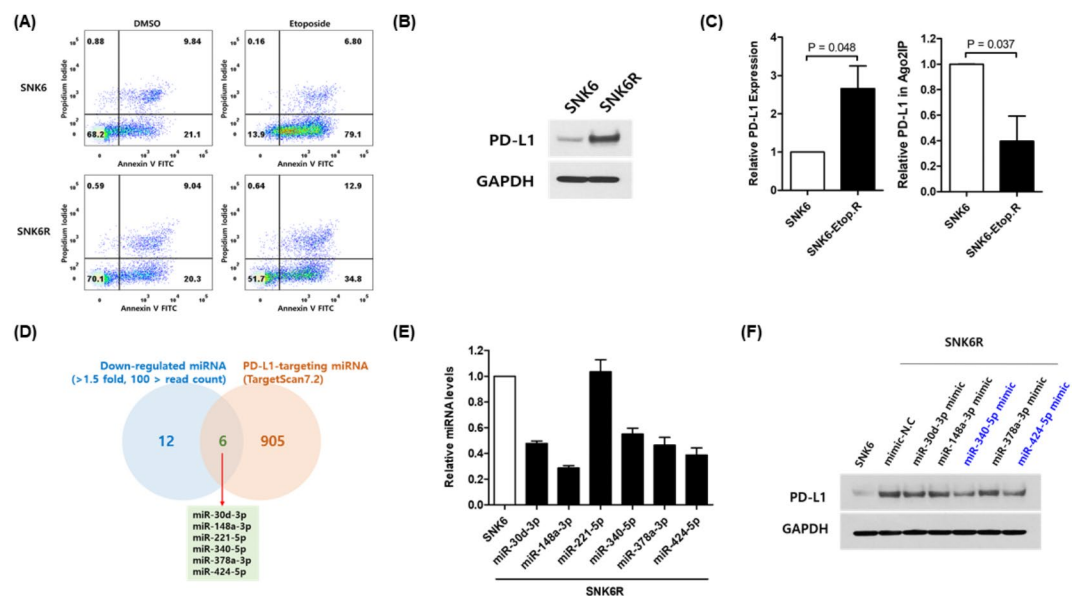


**Fig. 1.** MiR-340-5p and miR-424-5p are upregulated in etoposide-resistant ENKTL cells. (A) SNK6 and etoposide-resistant SNK6 (SNK6R) cells were treated with etoposide (2  $\mu$ M) for 72 h, followed by the apoptosis assay. (B) Increased expression of PD-L1 was observed in SNK6R cells. (C) The expression and enrichment of PD-L1 mRNA in Ago2 RIP were assessed by RT-qPCR. (D) Six putative miRNAs were screened by comparing downregulated miRNAs obtained from RNA sequencing with a list of predicted PD-L1-targeting miRNAs. The binding sites between PD-L1 and these miRNAs were predicted by the TargetScan. (E) RT-qPCR analysis verified the decrease in expression levels of candidate miRNAs in SNK6 and SNK6R cells. (F) Western blot analysis of PD-L1 was performed on SNK6 cells transfected with six miRNA mimics (miR-30d-3p, miR-148a-3p, miR-340-5p, miR-378a-3p, and miR-424-5p) and a negative control. Relative expressions were determined using the 2 $^{-\Delta\Delta CT}$  method, with U6 as a housekeeping gene for miRNAs, and 18 S rRNA and glyceraldehyde-3-phosphate dehydrogenase (GAPDH) for PD-L1 mRNA. Data represent mean  $\pm$  SEM ( $n = 3$ ).

## Exploring the regulation of PD-L1 by miR-340-5p and miR-424-5p in ENKTL cells

To elucidate how miR-340-5p and miR-424-5p modulate PD-L1 expression, we manipulated these miRNAs in ENKTL cells through the transfection of inhibitors and mimics. Transfection of SNK6 cells with miRNA inhibitors of miR-340-5p or miR-424-5p led to an increase in PD-L1 protein levels (Fig. 2A). In contrast, overexpression of miR-340-5p or miR-424-5p by miRNA mimic decreased the levels of PD-L1 protein (Fig. 2B) and mRNA (Fig. 2C) in SNK6R cells. The direct interaction between these miRNAs and the 3'UTR of PD-L1 mRNA was examined by Ago2 RNP-IP and luciferase reporter assay. Results from Ago2 RNP-IP revealed that the enrichment of PD-L1 mRNA in Ago2 IP was enhanced by increasing the levels of miR-340-5p or miR-424-5p, demonstrating that these miRNAs are involved in the regulation of PD-L1 (Fig. 2D). To validate the direct binding and functional impact of these miRNAs on PD-L1 expression, we employed dual-luciferase reporter assays. We constructed luciferase vectors containing the 3'-UTR sequences of PD-L1 mRNA that are targeted by miR-340-5p and miR-424-5p, along with vectors containing mutated sequences in the seed regions of these miRNAs. The assays demonstrated that both miRNAs suppressed luciferase activity when paired with the wild-type seed sequence; however, this suppression was abolished when mutations were introduced into the seed regions, disrupting the direct binding (Fig. 2E and F). These findings collectively confirm that miR-340-5p and miR-424-5p regulate PD-L1 expression by directly binding to the 3'UTR of PD-L1 mRNA, significantly influencing the expression of this critical immunological checkpoint in ENKTL cells.

## Correlation of miRNAs with PD-L1 in ENKTL patients

To investigate the relationship between miRNA expression levels and the CPS of PD-L1 in patients, we performed immunohistochemistry and RT-qPCR assays on biopsy specimens from three patients. These patients exhibited varying CPS of PD-L1: one with a CPS of 100 (Pt1), one with a CPS of 30 (Pt2), and one with a CPS of 0 (Pt3; Fig. 3A). In comparing miR-340-5p expression levels with PD-L1 expression in tumor tissues from three patient samples, patients with low (Pt2) and absent (Pt3) PD-L1 expression showed significantly higher miR-340-5p levels compared to the patient with high PD-L1 expression (Pt1; Fig. 3B). This suggests a potential inhibitory effect of miR-340-5p on PD-L1 expression in tumor tissues. Similarly, serum miR-340-5p levels were reduced in the patient with high PD-L1 expression (Pt1) compared to those with lower PD-L1 expression (Pt2 and Pt3; Fig. 3C). Conversely, the expression of miR-424-5p in tumor tissues did not demonstrate a significant variation correlating with PD-L1 expression levels (Fig. 3B), and serum levels of miR-424-5p was not related to tissue PD-L1 expression (Fig. 3C). To corroborate these observations, we extended our analysis to include serum samples from 16 patients, who had corresponding CPS data for PD-L1 expression in their tumor tissues (Supplementary Fig. 1). The expanded analysis revealed a negative correlation between the levels of miR-340-5p and CPS,

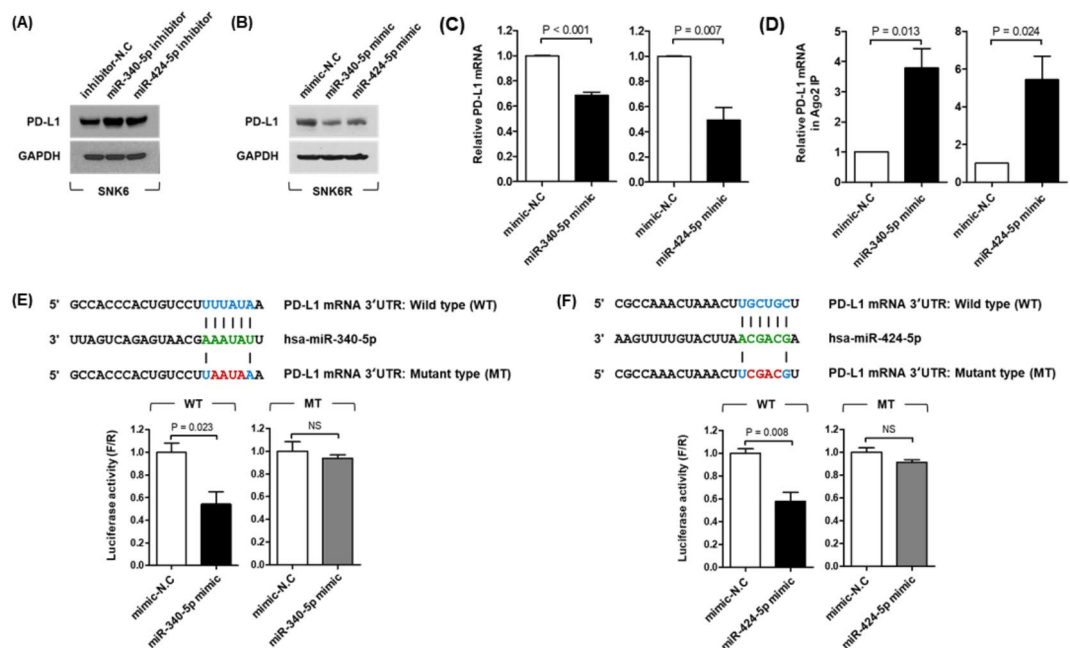


**Fig. 2.** MIR-340-5p and miR-424-5p directly target the PD-L1. Following the transfection of SNK6 and SNK6R cells with miR-340-5p and miR-424-5p inhibitors or mimics, the expression levels of PD-L1 protein (A and B) and mRNA (C) were determined by western blot and RT-qPCR, respectively. (D) After overexpression of miR-340-5p or miR-424-5p, the enrichment of PD-L1 mRNA was examined using Ago2 IP, assessed by RT-PCR. (E and F) The schematic diagram showed the binding sites of miR-340-5p and miR-424-5p on the 3'UTR of PD-L1. Luciferase reporter assays were conducted on cells co-transfected with a reporter construct containing either the wild-type (WT) or mutant (MU) 3'UTR of PD-L1 and the miR-340-5p and miR-424-5p mimics or mimic-NC. Luciferase expression was measured using a Dual-GLO™ Luciferase Assay System. Data represent mean ± SEM. All experiments were repeated three times.

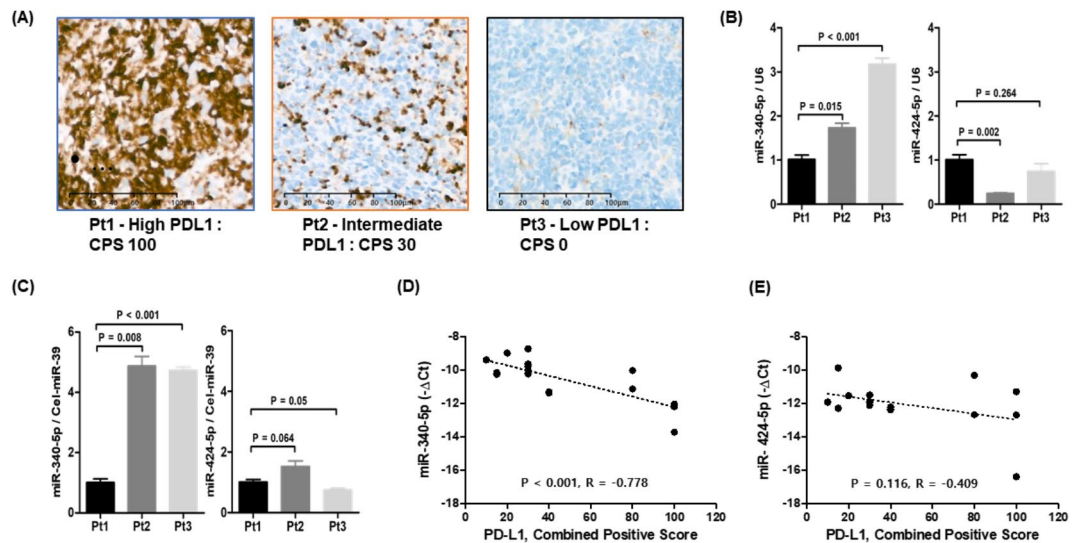


**Fig. 3.** A negative correlation between miR-340-5p and miR-424-5p and PD-L1 expression in ENKTL samples. **(A)** Representative images of immunohistochemical stains showing patterns of PD-L1 expression in three patients with CPS score of 100 (Pt1, high), 30 (Pt2, intermediate), and 0 (Pt3, low). **(B)** The expression levels of miR-340-5p and miR-424-5p were lower in tumor tissue of patients (Pt1, Pt2) with high and intermediate PD-L1 expression than a patient with low PD-L1 expression (Pt3). The U6 served as the corresponding internal reference for cellular miRNA. **(C)** The expression levels of miR-340-5p and miR-424-5p in the serum of the same patient were confirmed by RT-qPCR. The synthetic spike control cel-miR-39 was used as an invariant control for the serum miRNA. **(D, E)** A negative correlation between miR-340-5p or miR-424-5p and PD-L1 CPS in the ENKTL tissues.

indicating that higher levels of miR-340-5p are associated with lower CPS values of PD-L1 (Fig. 3D). In contrast, no significant relationship was identified between miR-424-5p levels and the CPS of PD-L1 (Fig. 3E).

### Association of miR-340-5p with soluble PD-L1 and response to pembrolizumab

Based on the findings indicating an association between serum and tissue levels of miR-340-5p and PD-L1 expression, we extended our analysis to investigate the relationship between serum miR-340-5p levels and soluble PD-L1 in 38 patients, for whom a correlation between tissue and soluble PD-L1 expression was observed (Supplementary Fig. 2). There was a significant negative correlation between serum levels of miR-340-5p and soluble PD-L1, with higher miRNA levels corresponding to lower soluble PD-L1 levels (Fig. 4A). To explore the association of serum levels of miR-340-5p with response to pembrolizumab, we categorized 19 patients who had serum samples available for analysis that were archived prior to pembrolizumab treatment based on their response: complete response (CR), partial response (PR), or progressive disease (PD). Notably, miR-340-5p levels were significantly lower in the PD group compared to the CR/PR group (Fig. 4B). The levels of soluble PD-L1 was also significantly different between responders and non-responders to pembrolizumab, despite the relatively small number of patients (Fig. 4C). We compared the serum levels of miR-340-5p with the response to pembrolizumab in 16 patients who received it as salvage therapy. Among these, all patients who achieved a complete response to pembrolizumab ( $n = 5$ ) had serum miR-340-5p levels below  $-10$ , whereas most non-responders ( $n = 11$ ) had levels above  $-10$ , with the exception of two patients (Fig. 4D). These findings suggest a potential association between serum miR-340-5p levels and the response to pembrolizumab, and this relationship highlights the potential utility of miR-340-5p as a biomarker for predicting response to pembrolizumab treatment and for assessing prognosis in patients with ENKTL (Fig. 4E).

### Discussion

The current treatment strategy for newly diagnosed ENKTL patients typically involves combination chemotherapy with or without radiotherapy, with most regimens incorporating multiple chemotherapeutic agents. However, ENKTL is inherently resistant to anthracyclines like doxorubicin, making non-anthracycline chemotherapy regimens the standard approach for treatment. L-asparaginase is a key component of many non-anthracycline chemotherapy combination regimens. Resistance to L-asparaginase, however, is primarily due to the development of neutralizing antibodies against this biologic agent, which is derived from bacterial sources. Therefore, the development of L-asparaginase-resistant tumor cells under prolonged in vitro exposure may not accurately reflect clinical treatment failure in ENKTL patients. On the other hand, etoposide is another commonly used agent, featured in regimens like SMILE (steroid, methotrexate, ifosfamide, L-asparaginase, and etoposide), VIPD (etoposide, ifosfamide, cisplatin and dexamethasone) and VIDL (etoposide, ifosfamide, dexamethasone and L-asparaginase)<sup>15–17</sup>. As a result, patients with ENKTL may be exposed to etoposide repeatedly throughout their treatment. This repeated exposure creates a clinical scenario conducive to the development of etoposide-



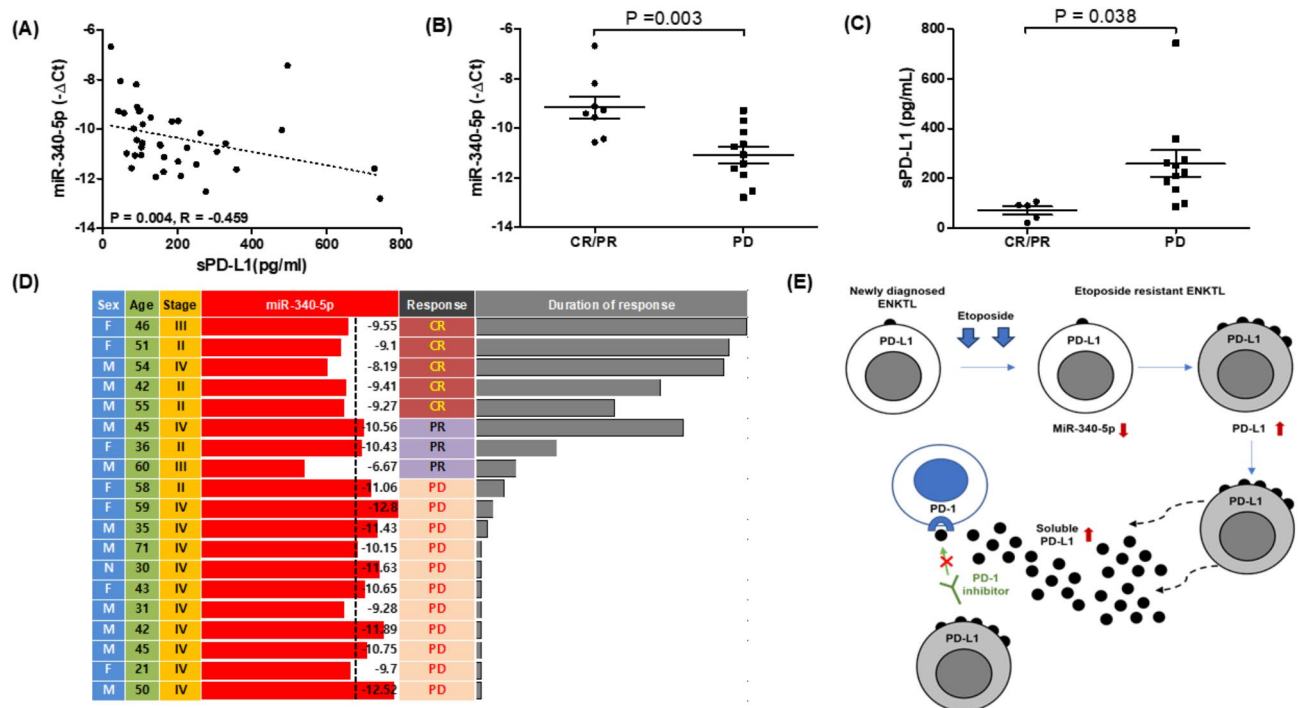


**Fig. 4.** Response to pembrolizumab and levels of miR-340-5p and miR-424-5p. **(A)** A negative correlation between miR-340-5p and soluble PD-L1 in the ENKTL. The expression of miR-340-5p **(B)** and soluble PD-L1 **(C)** levels in ENKTL patients with PD compared with those in CR/PR. **(D)** Swimmer plot indicating the duration of responses in 19 patients following treatment with pembrolizumab. **(E)** A schematic model illustrates the potential consequences of ICI resistance in ENKTL cells. Upregulation of PD-L1, caused by reduced miR-340-5p in etoposide-resistant ENKTL, may lead to an increase in soluble PD-L1 (sPD-L1). This increased sPD-L1 can bind to PD-1 on T cells, potentially inducing T-cell exhaustion and impairing the anti-tumor immune response.

resistant tumor cells. To better model this clinical reality, we developed an etoposide-resistant tumor cell line in this study.

PD-L1 expression on tumor cells is a critical mechanism by which cancer cells evade the immune system, with several pathways contributing to its regulation. Genetic and epigenetic alterations, such as amplification of the PD-L1 gene (*CD274*) or copy number alterations of chromosome 9p24.1, are notable mechanisms that enhance PD-L1 expression<sup>18</sup>. Inflammatory cytokines, particularly interferon-gamma (IFN- $\gamma$ ), also can induce PD-L1 expression by activating the JAK/STAT pathway. IFN- $\gamma$ , produced by activated T cells and NK cells, binds to its receptor on tumor cells, leading to this pathway's activation and subsequent PD-L1 transcription<sup>19</sup>.

PD-L1 expression could be upregulated in various cancers following exposure to chemotherapeutics, often correlating with poor prognosis<sup>20,21</sup>. Considering immune checkpoint inhibitors are used as salvage treatments for patients with relapsed or refractory diseases, repeated chemotherapy exposure might contribute to PD-L1 expression in heavily pre-treated cancer patients, including those with ENKTL. However, the response to immune checkpoint inhibitors in these patients has been unsatisfactory, despite documented PD-L1 expression, suggesting different underlying mechanisms of PD-L1 expression in relapsed or refractory ENKTL.

In our study, we focused on miRNAs that directly target and regulate PD-L1 mRNA in etoposide-resistant ENKTL cells. We identified miR-340-5p and miR-424-5p as key regulators of both PD-L1 mRNA and protein levels, confirmed through Ago2 RNP-IP and luciferase reporter assays. Although these miRNAs did not influence cell growth, proliferation, apoptosis, or drug response (data not shown), their modulation of PD-L1 expression suggests a potential impact on immune escape mechanisms. Among the two miRNAs, only miR-340-5p showed an inverse correlation with PD-L1 expression in clinical samples. Analysis revealed that miR-340-5p levels were significantly higher in PD-L1-negative ENKTL tissues compared to PD-L1-positive tissues, while miR-424-5p did not show a significant association (Fig. 3).

Furthermore, our expanded analysis demonstrated an inverse correlation between serum miR-340-5p levels and soluble PD-L1 levels, consistent with its relation to tissue PD-L1 expression (Fig. 4A). Soluble PD-L1, a biomarker for liquid biopsies, is related to histological PD-L1 expression in tumor tissue and is associated with poor prognosis in various cancers, including lymphomas<sup>22,23</sup>. Enhanced membrane-bound PD-L1 expression in tumor cells may increase circulating soluble PD-L1, potentially interfering with PD-1 inhibitors' efficacy. Consistently, low blood levels of miR-340-5p and high soluble PD-L1 were significantly associated with poor response to pembrolizumab and the duration of response in our study (Fig. 4).

In this study, we aimed to identify microRNAs that regulate PD-L1 expression in ENKTL, as PD-1 inhibitors, such as pembrolizumab, are currently recommended as standard salvage therapy for relapsed or refractory ENKTL patients previously treated with etoposide-containing chemotherapy. We identified miR-340-5p as a potential regulator of PD-L1 expression in ENKTL tumor cells, particularly in etoposide-resistant ENKTL, which reflects the clinical setting. Consequently, our study focused on investigating the effects of miR-340-5p on PD-L1 expression rather than its direct tumor-suppressive effects on proliferation, despite prior studies showing that miR-340-5p acts as a tumor suppressor across various cancer types by targeting multiple oncogenes involved in cancer cell proliferation, apoptosis, invasion, and metastasis such as *RhoA*, *ZNF503* and *ROCK*<sup>24,25</sup>, and several tumorigenesis-related signaling pathways, including AKT, JAK1/STAT3, and Wnt/ $\beta$ -catenin<sup>26,27</sup>. Given the scope of our study, we did not assess whether miR-340-5p inhibits proliferation or invasion of ENKTL. Although recent studies have demonstrated its tumor-suppressive role in inhibiting proliferation, migration, and invasion across various cancer types, limited data exist regarding its function in ENKTL. In cervical cancer, miRNAs including miR-340 regulate PD-L1 and serve as potential therapeutic targets that can inhibit cell proliferation and invasion, offering strategies to suppress metastatic phenotypes and counteract the immunosuppressive microenvironment<sup>28</sup>. Additionally, in diffuse large B-cell lymphoma, miR-340-5p influences CD8<sup>+</sup> T lymphocytes' functionality and antitumor functions, impacting the tumor microenvironment and presenting a novel target for immunotherapy<sup>29</sup>. This variability highlights the possibility that its role may differ across tumor types. These findings underscore miR-340-5p's potential as a predictive biomarker for immune checkpoint inhibitor efficacy and its role in modulating PD-L1 expression, with significant implications for therapeutic strategies.

However, this study has several limitations. First, we utilized only one cell line, SNK6, to develop an etoposide-resistant model and analyze miRNA profiles. Second, the analysis of the association between PD-L1 expression and serum miR-340-5p was conducted in a relatively small cohort of ENKTL patients due to the rarity of the disease. Additionally, the correlation between serum miR-340-5p levels and response to pembrolizumab was evaluated in a limited number of patients receiving this therapy. Accordingly, the small sample size in this study limits the ability to establish a robust cutoff value for miR-340-5p levels as a biomarker predicting the response to pembrolizumab. Therefore, further studies with larger patient cohorts and additional tumor cell lines are needed to validate our findings and define a reliable cutoff value.

In conclusion, our research indicates that miR-340-5p regulates PD-L1 and could be a valuable prognostic marker for treatment with immune checkpoint inhibitors. Assessing serum miR-340-5p levels prior to treatment may help tailor more effective use of immune checkpoint inhibitors, such as pembrolizumab, for patients with ENKTL. However, further studies with larger sample sizes are needed to confirm the potential of miR-340-5p as a predictive biomarker for treatment response in these patients.

## Materials and methods

### Cell culture

The SNK6 and SNK6R cells were maintained in RPMI-1640 medium, which was supplemented with 10% heat-inactivated fetal bovine serum. These cells also received recombinant human interleukin-2 (PeproTech in Rocky Hill, NJ, USA) to support their growth and viability. Additionally, the cells were treated with etoposide (Sigma-Aldrich in St Louis, MO, USA) to sustain their drug-resistant phenotype. SNK6 cell lines were obtained from Dr. Won seog Kim (Samsung medical center).

### Patients

Participants in our study were selected from a prospective cohort after providing written informed consent. The study focused on patients with relapsed or refractory ENKTL who underwent pembrolizumab therapy as a salvage treatment from May 2017 to March 2021 at Samsung medical center. The study was approved by the Samsung Medical Center Institutional Review Board of the ethics committee (IRB No. 2016-11-040). It was conducted in accordance with the ethical principles of the Declaration of Helsinki and the Korea Good Clinical Practice guidelines. Lymphoma pathology was confirmed by an expert, J.C., specializing in lymphoma, using immunohistochemistry and EBV in situ hybridization techniques<sup>30</sup>. Serum samples were serially collected from enrolled patients at diagnosis as well as during the follow-up. Thus, we preserved those serum samples at  $-80^{\circ}\text{C}$  for future analysis including serum samples obtained prior to pembrolizumab administration.

### RNA isolation and gene expression analysis procedures

Total RNA was extracted using the Qiagen RNA extraction kit (Qiagen, Valencia, CA, USA), following the manufacturer's guidelines. Subsequently, 1  $\mu\text{g}$  of this RNA was reverse-transcribed into cDNA using the Omniscript RT kit (Qiagen). For quantitative gene expression analysis, real-time PCR was conducted on a QuantStudio6 system (Applied Biosystems, Foster, CA, USA) using SYBR Green PCR Master Mix (Thermo Fisher Scientific, Waltham, MA, USA). For miRNA expression, 10 ng of RNA was processed with the TaqMan MicroRNA Reverse Transcription Kit (Thermo Fisher Scientific), incorporating specific miRNA primers. The resulting cDNA was then diluted and amplified using TaqMan Universal Master Mix II and TaqMan microRNA Expression Assays specific to each target miRNA, such as hsa-miR-340-5p and hsa-miR-424-5p. Expression levels of miRNA and mRNA were normalized to internal controls U6 and GAPDH, respectively, and the relative expression was quantified using the  $2^{-\Delta\Delta\text{CT}}$  method.

### RNA sequencing and differential gene expression analysis

Total RNA was processed for sequencing library construction using the KAPA Library Quantification kits as specified in the manufacturer's protocol. The prepared indexed libraries were sequenced on an Illumina HiSeq 2500 system (Illumina, Inc., San Diego, CA, USA) by Macrogen Incorporated, employing single-end sequencing

with a read length of 51 base pairs. Differential gene expression analysis was conducted using edgeR v3.40.2 (Robinson, Mark D. et al., 2010), which utilized raw sequencing counts. Statistical significance of the gene expression data was adjusted using the Benjamini-Hochberg algorithm to control the false discovery rate (FDR). Genes were considered significantly differentially expressed if they met the criteria of having an absolute fold change of at least 1.5 and a raw p-value below 0.05.

### Apoptosis assay via annexin-V-FITC and flow cytometry

Apoptosis in SNK6 and SNK6R cells was assessed using an Annexin-V-fluorescein isothiocyanate (FITC) Apoptosis Detection Kit (BD Biosciences, San Jose, CA, USA). Following exposure to etoposide, cells were collected and stained according to the protocol provided by the manufacturer. The stained cells were then analyzed using a BD FACS Lyric flow cytometry system (BD Biosciences) to quantify apoptotic cells.

### Protein extraction and western blot analysis

Total protein was extracted from cells using RIPA buffer containing 0.5% sodium deoxycholate, 1% Nonidet P-40, 150 mM NaCl, 50 mM Tris (pH 7.5), 0.1% sodium dodecyl sulfate (SDS), 1 mM phenylmethylsulfonyl fluoride (PMSF), and complete protease and phosphatase inhibitors. The lysates were then cleared by microcentrifugation at 13,000 rpm for 20 min at 4 °C. Protein concentration was determined using the Pierce BCA Protein Assay Kit (Thermo Fisher Scientific). For Western blot analysis, proteins were separated on a 4–12% SDS polyacrylamide gel and subsequently transferred to nitrocellulose membranes. Membranes were blocked with 5% nonfat milk at room temperature and incubated overnight at 4 °C with primary antibodies targeting PD-L1 (Cell Signaling, Danvers, MA, USA) and GAPDH (Santa Cruz Biotechnology, Dallas, TX, USA). After washing with TBST buffer (50 mM Tris [pH 7.5], 150 mM NaCl, 0.05% Tween 20), the membranes were incubated with HRP-conjugated secondary antibodies (Cell Signaling Technology) for 1 h at room temperature. Protein bands were visualized using enhanced chemiluminescence (Thermo Fisher Scientific).

### Ribonucleoprotein immunoprecipitation (RNP-IP) using Ago2 antibody

For the RNP-IP, Dynabeads<sup>®</sup> Protein G (Thermo Fisher Scientific) were first coated with either control IgG (Santa Cruz Biotechnology) or an Ago2 antibody (Sigma). To prepare the cytoplasmic lysates, cells were lysed using a protein extraction buffer (PEB) composed of 20 mM Tris-HCl pH 7.4, 0.5% NP-40, 100 mM KCl, 5 mM MgCl<sub>2</sub>, supplemented with protease/phosphatase inhibitors and RNaseOUT (Invitrogen, Carlsbad, CA, USA). Equal amounts of these lysates were then incubated with the antibody-coated Dynabeads for 4 h at 4 °C. Following incubation, the beads were washed several times with NT2 buffer. The Ago2-immunoprecipitated (IP) materials were then treated with DNase I (Ambion, Austin, TX, USA) and proteinase K at 55 °C (Invitrogen) for 20 min to digest DNA and proteins. Subsequently, the RNA was isolated using acid phenol (Ambion) and precipitated using absolute ethanol overnight at –20 °C. The relative levels of mRNA associated with the Ago2-containing RNA-induced silencing complex (RISC) were quantified using RT-qPCR, as previously described. The expression levels were normalized to 18 S RNA to ensure accurate quantification.

### Assessing miRNA targeting via dual-luciferase reporter assay

To investigate the direct binding of miR-340-5p and miR-424-5p to the 3'-untranslated region (UTR) of PD-L1 mRNA, constructs were prepared using the pmirGLO dual-luciferase vector (Promega, Madison, WI, USA). These constructs included both Wild-type or mutated sequences of the miRNA response elements for miR-340-5p (Forward primer: 5'-ATCTGGTTCCGCGTGGATGAAGGGAGACAGCAGACATCTGAATG-3'; Reverse primer: 5'-TCACGATGCGGCCGCTCGAGTATTCACAGGCAAAGTAGTCCTTCAAG-3'), and for miR-424-5p (Forward primer: 5'-ATCTGGTTCCGCGTGGATCCATGAAGGGAGACAGCAGACATCTGAA TG-3'; Reverse primer: 5'-TCACGATGCGGCCGCTCGAGCTATTCACAGGCAAAGTAGTCCTTCAAG-3'). Cells were transfected with 50 nM of either control miRNA or mimics of miR-340-5p and miR-424-5p and subsequently seeded into 24-well plates. The following day, these cells were transfected with 100 ng of either the wild-type or mutant luciferase vectors. After 24 h post-transfection, luciferase activity was measured using the Dual-Luciferase Reporter Assay System (Promega). The activity of firefly luciferase was normalized against Renilla luciferase to assess the relative reporter gene expression, which indicates miRNA binding and regulation efficacy.

### Immunohistochemistry for PD-L1

Immunohistochemistry was performed for PD-L1 with Rabbit Anti-Human PD-L1/CD274 Monoclonal Antibody (Clone SP142) as previously described<sup>31</sup>. Tumor cells expressing PD-L1 and PD-L1-positive tumor-associated macrophages (TAMs) were evaluated because the expression of PD-L1 in TAMs was reported in ENKTL<sup>32</sup>. To represent the extent of PD-L1 expression where tumor cells were present, the percentage of total PD-L1-positive cells including PD-L1-positive tumor cells and TAMs among tumor cells was calculated as a Combined Positive Score (CPS) for PD-L1 score.

### Measurement of soluble PD-L1 levels by ELISA

Soluble PD-L1 levels were quantified using the PD-L1/B7-H1 Quantikine ELISA Kit (R&D Systems, Minneapolis, MN, USA). The procedure began with the addition of 100 µL of both standards and samples into the assay wells, followed by a 2 h incubation at room temperature. After this initial incubation, the wells were washed four times to remove unbound substances. Subsequently, a B7-H1 conjugate was added to each well, followed by another 2 h incubation at room temperature. After another round of washing, a substrate solution was introduced to the wells and allowed to incubate for 30 min in the dark to facilitate the development of color. The reaction was

halted by adding a stop solution. Finally, the optical density of each well was determined using a Spectramax microplate reader set to a wavelength of 450 nm (ABS Plus, CA, USA).

## Data presentation and statistical analysis

Data from the study are presented as the mean  $\pm$  standard error of the mean (SEM). Cell-based experiments were conducted in triplicate and each experiment was independently repeated at least three times to ensure reproducibility and reliability of the results. Statistical analyses were performed using IBM PASW version 25.0 software program (IBM SPSS Inc., Armonk, NY, USA). For the statistical comparison of data between two groups, an Independent Samples t-test was utilized. A p-value of less than 0.05 was considered statistically significant.

## Data availability

The raw sequence data reported in this paper have been deposited in the Genome Sequence Archive (Genomics, Proteomics & Bioinformatics 2021) in National Genomics Data Center (Nucleic Acids Res 2022), China National Center for Bioinformation / Beijing Institute of Genomics, Chinese Academy of Sciences (GSA-Human: HRA007323) that are publicly accessible at <https://ngdc.cnbc.ac.cn/gsa-human>.

Received: 8 November 2024; Accepted: 13 February 2025

Published online: 25 February 2025

## References

1. Tse, E. & Kwong, Y. L. The diagnosis and management of NK/T-cell lymphomas. *J. Hematol. Oncol.* **10**, 85. <https://doi.org/10.1186/s13045-017-0452-9> (2017).
2. Chen, B. J. et al. PD-L1 expression is characteristic of a subset of aggressive B-cell lymphomas and virus-associated malignancies. *Clin. Cancer Res.* **19**, 3462–3473. <https://doi.org/10.1158/1078-0432.Ccr-13-0855> (2013).
3. Darvin, P., Toor, S. M., Nair, S., Elkord, E. & V. & Immune checkpoint inhibitors: Recent progress and potential biomarkers. *Exp. Mol. Med.* **50**, 1–11. <https://doi.org/10.1038/s12276-018-0191-1> (2018).
4. Kim, S. J., Hyeon, J., Cho, I., Ko, Y. H. & Kim, W. S. Comparison of efficacy of pembrolizumab between epstein-barr virus-positive and -negative relapsed or refractory non-hodgkin lymphomas. *Cancer Res. Treat.* **51**, 611–622. <https://doi.org/10.4143/crt.2018.191> (2019).
5. Li, X. et al. Activity of pembrolizumab in relapsed/refractory NK/T-cell lymphoma. *J. Hematol. Oncol.* **11**, 15. <https://doi.org/10.1186/s13045-018-0559-7> (2018).
6. Kim, S. J. et al. Exosomal and soluble programmed death-ligand 1 (PD-L1) predicts responses to pembrolizumab in patients with extranodal NK/T-Cell lymphoma. *Cancers (Basel)* **14**. <https://doi.org/10.3390/cancers14225618> (2022).
7. Yang, Y. et al. Exosomal PD-L1 harbors active defense function to suppress T cell killing of breast cancer cells and promote tumor growth. *Cell. Res.* **28**, 862–864. <https://doi.org/10.1038/s41422-018-0060-4> (2018).
8. Theodoraki, M. N., Yerneni, S. S., Hoffmann, T. K., Gooding, W. E. & Whiteside, T. L. Clinical significance of PD-L1(+) exosomes in plasma of head and neck cancer patients. *Clin. Cancer Res.* **24**, 896–905. <https://doi.org/10.1158/1078-0432.CCR-17-2664> (2018).
9. Wang, Q. et al. The roles of microRNAs in regulating the expression of PD-1/PD-L1 immune checkpoint. *Int. J. Mol. Sci.* **18** <https://doi.org/10.3390/ijms18122540> (2017).
10. Fujita, Y. et al. The clinical relevance of the miR-197/CKS1B/STAT3-mediated PD-L1 network in chemoresistant non-small-cell lung cancer. *Mol. Ther.* **23**, 717–727. <https://doi.org/10.1038/mt.2015.10> (2015).
11. Zhao, L. et al. The tumor suppressor mir-138-5p targets PD-L1 in colorectal cancer. *Oncotarget* **7**, 45370–45384. <https://doi.org/10.18632/oncotarget.9659> (2016).
12. Wang, X. et al. Tumor suppressor miR-34a targets PD-L1 and functions as a potential immunotherapeutic target in acute myeloid leukemia. *Cell. Signal.* **27**, 443–452. <https://doi.org/10.1016/j.cellsig.2014.12.003> (2015).
13. Katakura, S. et al. MicroRNA-200b is a potential biomarker of the expression of PD-L1 in patients with lung cancer. *Thorac. Cancer* **11**, 2975–2982. <https://doi.org/10.1111/1759-7714.13653> (2020).
14. Ryu, K. J. et al. Serum-derived exosomal MicroRNA profiles can predict poor survival outcomes in patients with extranodal natural killer/T-cell lymphoma. *Cancers (Basel)* **12**. <https://doi.org/10.3390/cancers12123548> (2020).
15. Kwong, Y. L. et al. SMILE for natural killer/T-cell lymphoma: Analysis of safety and efficacy from the Asia lymphoma study group. *Blood* **120**, 2973–2980. <https://doi.org/10.1182/blood-2012-05-431460> (2012).
16. Kim, S. J. et al. Phase II trial of concurrent radiation and weekly cisplatin followed by VIPD chemotherapy in newly diagnosed, stage IE to IIE, nasal, extranodal NK/T-cell lymphoma: Consortium for Improving survival of lymphoma study. *J. Clin. Oncol.* **27**, 6027–6032. <https://doi.org/10.1200/JCO.2009.23.8592> (2009).
17. Kim, S. J. et al. Concurrent chemoradiotherapy followed by L-asparaginase-containing chemotherapy, VIDL, for localized nasal extranodal NK/T cell lymphoma: CISL08-01 phase II study. *Ann. Hematol.* **93**, 1895–1901. <https://doi.org/10.1007/s00277-014-2137-6> (2014).
18. Zanelli, M. et al. Programmed death Ligand 1 (PD-L1) expression in Lymphomas: state of the art. *Int. J. Mol. Sci.* **25** <https://doi.org/10.3390/ijms25126447> (2024).
19. Garcia-Diaz, A. et al. Interferon receptor signaling pathways regulating PD-L1 and PD-L2 expression. *Cell. Rep.* **19**, 1189–1201. <https://doi.org/10.1016/j.celrep.2017.04.031> (2017).
20. Gilad, Y. et al. Drug-induced PD-L1 expression and cell stress response in breast cancer cells can be balanced by drug combination. *Sci. Rep.* **9**, 15099. <https://doi.org/10.1038/s41598-019-51537-7> (2019).
21. Ng, H. Y. et al. Chemotherapeutic treatments increase PD-L1 expression in Esophageal squamous cell carcinoma through EGFR/ERK activation. *Transl. Oncol.* **11**, 1323–1333. <https://doi.org/10.1016/j.tranon.2018.08.005> (2018).
22. Rossille, D. et al. High level of soluble programmed cell death ligand 1 in blood impacts overall survival in aggressive diffuse large B-Cell lymphoma: Results from a French multicenter clinical trial. *Leukemia* **28**, 2367–2375. <https://doi.org/10.1038/leu.2014.137> (2014).
23. Cho, I. et al. Serum levels of soluble programmed death-ligand 1 (sPD-L1) in patients with primary central nervous system diffuse large B-cell lymphoma. *BMC Cancer* **20**, 120. <https://doi.org/10.1186/s12885-020-6612-2> (2020).
24. Lu, G. & Zhang, Y. MicroRNA-340-5p suppresses non-small cell lung cancer cell growth and metastasis by targeting ZNF503. *Cell. Mol. Biol. Lett.* **24**, 34. <https://doi.org/10.1186/s11658-019-0161-1> (2019).
25. Maskey, N. et al. MicroRNA-340 inhibits invasion and metastasis by downregulating ROCK1 in breast cancer cells. *Oncol. Lett.* **14**, 2261–2267. <https://doi.org/10.3892/ol.2017.6439> (2017).



26. Yu, J. et al. miR-340 inhibits proliferation and induces apoptosis in gastric cancer cell line SGC-7901, possibly via the AKT pathway. *Med. Sci. Monit.* **23**, 71–77. <https://doi.org/10.12659/msm.898449> (2017).
27. Rongxin, S., Pengfei, L., Li, S., Xiaochen, J. & Yihe, H. MicroRNA-340-5p suppresses osteosarcoma development by down-regulating the Wnt/ $\beta$ -catenin signaling pathway via targeting the STAT3 gene. *Eur. Rev. Med. Pharmacol. Sci.* **23**, 982–991. [https://doi.org/10.26355/eurrev\\_201902\\_16985](https://doi.org/10.26355/eurrev_201902_16985) (2019).
28. Dong, P. et al. Control of PD-L1 expression by miR-140/142/340/383 and oncogenic activation of the OCT4-miR-18a pathway in cervical cancer. *Oncogene* **37**, 5257–5268. <https://doi.org/10.1038/s41388-018-0347-4> (2018).
29. Xu, Y. et al. MiRNA-340-5p mediates the functional and infiltrative promotion of tumor-infiltrating CD8(+) T lymphocytes in human diffuse large B cell lymphoma. *J. Exp. Clin. Cancer Res.* **39**, 238. <https://doi.org/10.1186/s13046-020-01752-2> (2020).
30. Cho, J. Basic immunohistochemistry for lymphoma diagnosis. *Blood Res.* **57**, 55–61. <https://doi.org/10.5045/br.2022.2022037> (2022).
31. Cho, J. et al. Immune subtyping of extranodal NK/T-cell lymphoma: A new biomarker and an immune shift during disease progression. *Mod. Pathol.* **33**, 603–615. <https://doi.org/10.1038/s41379-019-0392-8> (2020).
32. Nagato, T. et al. Programmed death-ligand 1 and its soluble form are highly expressed in nasal natural killer/T-cell lymphoma: A potential rationale for immunotherapy. *Cancer Immunol. Immunother.* **66**, 877–890. <https://doi.org/10.1007/s00262-017-1987-x> (2017).

## Acknowledgements

We acknowledge all participants in this study and the Basic Science Research Program through the National Research Foundation of Korea (NRF) funded by the Ministry of Education (RS-2022-NR074971), by the Ministry of Science and ICT (RS-2023-NR077098).

## Author contributions

S.J.K. and H.H.K. conceived and designed the study. K.J.R., and H.J. wrote the manuscript. K.J.R., H.J., and B.P. performed the experiments. S.E.Y., C.P., W.S.K., and S.J.K. analyzed the data. All authors edited the manuscript and approved the final version of the manuscript.

## Declarations

## Competing interests

The authors declare no competing interests.

## Additional information

**Supplementary Information** The online version contains supplementary material available at <https://doi.org/10.1038/s41598-025-90542-x>.

**Correspondence** and requests for materials should be addressed to H.H.K. or S.J.K.

**Reprints and permissions information** is available at [www.nature.com/reprints](http://www.nature.com/reprints).

**Publisher's note** Springer Nature remains neutral with regard to jurisdictional claims in published maps and institutional affiliations.

**Open Access** This article is licensed under a Creative Commons Attribution-NonCommercial-NoDerivatives 4.0 International License, which permits any non-commercial use, sharing, distribution and reproduction in any medium or format, as long as you give appropriate credit to the original author(s) and the source, provide a link to the Creative Commons licence, and indicate if you modified the licensed material. You do not have permission under this licence to share adapted material derived from this article or parts of it. The images or other third party material in this article are included in the article's Creative Commons licence, unless indicated otherwise in a credit line to the material. If material is not included in the article's Creative Commons licence and your intended use is not permitted by statutory regulation or exceeds the permitted use, you will need to obtain permission directly from the copyright holder. To view a copy of this licence, visit <http://creativecommons.org/licenses/by-nc-nd/4.0/>.

© The Author(s) 2025